Measurement 122 (2018) 57–65

Contents lists available at ScienceDirect

Measurement

journal homepage: www.elsevier.com/locate/measurement

Pipeline corrosion and leakage monitoring based on the distributed optical fiber sensing technology

Liang Ren[a], Tao Jiang[a,*], Zi-guang Jia[b], Dong-sheng Li[a], Chao-lin Yuan[a], Hong-nan Li[a,c]

[a] School of Civil and Hydraulic Engineering, Dalian University of Technology, Dalian 116024, China
[b] School of Ocean Science and Technology, Dalian University of Technology, Panjin 124221, China
[c] School of Civil Engineering, Shenyang Jianzhu University, Shenyang 110168, China

ARTICLE INFO

Keywords:
Pipeline
Optical fiber sensor
Corrosion
Leakage
Monitoring

ABSTRACT

Pipeline is an important structure to transport oil and gas through long distances. However, pipeline also suffers from many threats especially corrosion and leakage. Therefore, it is necessary to conduct pipeline safety monitoring. With the advantage of high precision in distributed strain measurement, the optical frequency domain reflectometry (OFDR) technique is more suitable for pipeline monitoring. In this paper, a new application of the OFDR technique is introduced to monitor both corrosion and leakage. In order to verify this method, simulation tests of corrosion and leakage were conducted. In the corrosion test, several optical fiber sensors were bonded to the pipe surface with the same interval, forming a sensor array. Based on the sensor array, a hoop strain nephogram was created to show the corrosion level and corrosion location. In the leakage test, the results indicated that pipeline leakage can be detected by the distributed optical fiber sensor (DOFS). All the test results demonstrate that it is possible to monitor pipeline corrosion and leakage based on the hoop strain theory and the DOFS.

1. Introduction

Underground pipelines constitute one of the most important ways to transport large amounts of oil and gas through long distances [1,2]. Leakages in pipelines are very dangerous since they may lead to significant pollution of the environment [3,4], even severe safety accidents. Many factors, such as corrosion [5–7], vibration [8], and external impacts [9,10], may cause pipeline leakages. Among these factors, internal corrosion is one of the major problems that contribute to accidental events in pipelines since all pipelines are associated with the chlorides and sulfides in the products they carry [11]. Traditional pipeline internal detection mainly depends on the periodical inspection conducted by the pipeline inspection robot [12,13]. However, the periodical inspection does not provide real-time monitoring of the pipelines. As a result, a leakage may not be found in time and may cause much larger economic loss and environmental pollution [14]. Therefore, it is important to monitor the pipeline infrastructures in real time. Recently there are many methods developed for monitoring pipeline leakage by using various sensors, including distributed fiber optic sensing [15,16], piezoceramic transducers [17–19], acoustic emission (AE) transducers [20,21]. To help to effectively analyze the collected data by the sensors to extract the leakage information, various algorithms, such as SVM-based methods [22,23], Karman filtering [24], time-reversal enabled methods [25,26], standing wave difference methods [27], and wavelet analysis methods [28], have been developed.

Generally, oil and gas pipelines extend hundreds of kilometers [29]. Therefore, some traditional measuring techniques are inappropriate to use for the pipeline monitoring. For example, electromagnetic-based sensors, limited by larger loss in the process of electrical signal transmission, are not suitable for monitoring these long distance pipelines. Additionally, the electromagnetic-based sensors are prone to causing fire and explosion accidents to gas and oil pipelines.

Whereas, the optical fiber sensors (OFS) [30,31], which have proven their capabilities such as superior immunity to electromagnetic interference [32], long distance transmission [33], reliability and survivability in various environmental conditions, are ideal in pipeline applications [34]. According to the sensing technology, the OFS can be divided into two categories: distributed sensing and multipoint localized sensing. With the advantage of high precision, local fiber optic sensors are more suitable for measuring the degree of corrosion where the sensors locate at [35,36]. Distributed fiber optic sensing has the capability of measuring temperatures [37] and strains [38] at thousands of points along a single fiber. It is suitable for the monitoring

* Corresponding author.
E-mail address: jiangtao@mail.dlut.edu.cn (T. Jiang).

https://doi.org/10.1016/j.measurement.2018.03.018
Received 28 July 2017; Received in revised form 24 January 2018; Accepted 5 March 2018
Available online 07 March 2018
0263-2241/

damage, corrosion and leakage of pipeline structures [39,40]. With regard to damage or corrosion monitoring, Zou et al. utilized distributed Brillouin scattering sensor to identify several inner wall cutouts in an end-capped steel pipe by measuring the axial and hoop strain distributions along the outer surface of the pipe [41]; based on metal coated polymer-clad fiber optic cables, Alhandawi et al. developed a novel distributed sensor to detect the internal corrosion of pipeline [42]; Martins-Filho proposed and demonstrated an optical fiber sensor for testing the corrosion process in metal using the optical time domain reflectometry (OTDR) technique [43]. However, the widely applied distributed optic fiber sensor has its own advantages and limitations. For example, OTDR based technique has distributed measurement over a long distance due to its larger dynamic range, while its spatial resolution is usually on the order of meters to tens of meters [44], and its measurement accuracy is not high. Generally, the distributed sensors are more suitable for localizing damage or leakage instead of measuring the degree of damage or corrosion [45]. For pipeline leakage monitoring, some physical and chemical properties will change around the leakage point, such as temperature [46]. Monitoring of temperature profiles over long distance by means of Brillouin-based techniques represents a highly efficient way to perform leakage detection along pipelines [47]. An optical fiber distributed temperature sensing system, proposed by Tanimola et al., can detect leaks within 10 s of leaks occurring and locate leaks within 1–2 m of the leakage [48]. The presence of hydrocarbons also affects the optical properties of optical fiber, providing another means of detecting gas leaks. The leakage location and leaked gas concentration can be also detected using fiber optic sensing [49].

It can be concluded that a lot of studies have been conducted to solve the problems of pipeline corrosion and leakage monitoring according to the distributed fiber optical sensing technology. However, the existing OFS based monitoring technique can only implement corrosion monitoring or leakage monitoring. The OFDR technique with its superiority of high spatial resolution and high precision in distributed strain measurement, provides an effective approach for pipeline health monitoring [50]. Based on the advantages of OFDR technique in distributed strain measurement, a new application was proposed in this paper to monitor pipeline internal corrosion and leakage. Model tests were conducted to verify the monitoring method.

2. OFDR-based distributed sensing

The physical length and index of refraction of the fiber are intrinsically sensitive to environmental parameters, such as temperature and strain. In most practical cases, the spectral response of the Rayleigh backscatter will be determined by the effects of strain [51] and temperature [52]. OFDR technique, in essence, utilizes swept-wavelength interferometry to measure the Rayleigh backscatter as a function of position in the optical fiber [53]. Distributed strain data was acquired from the sensing optic fiber via an OFDR-based interrogator from LUNA Technologies (ODiSI-B model) with a spatial resolution of 5 mm and a measurement precision of ± 5 micro-strains [54]. Thus, any position of the sensing fiber can be used to measure the strain and temperature, similar to the optic fiber etched with continuous distributed FBG sensors [55].

3. Theory of pipeline health monitoring

3.1. Hoop strain measurement theory

The cross section of a long distance pipe expands uniformly under working pressure, causing the strain along the circumferential direction, called hoop strain. According to the theory of Material Mechanics, the relationship between the hoop strain ε and the pipeline internal pressure p is established.

$$\varepsilon = \frac{pR}{E\delta} \tag{1}$$

where E represents the Young's modulus of the pipe, δ represents the pipe wall thickness and R represents the radius of the pipe.

3.2. Corrosion monitoring based on hoop strain

The radius R and the Young's modulus E of the pipeline are constant. For the pipeline in normal conditions, P is a constant since pipelines usually work in a steady pressure. Therefore, the hoop strain ε is inversely proportional to the pipe wall thickness δ. Based on this principle, the measured circumferential strain variation can be used to estimate the wall thickness deduction, which is the most direct phenomenon caused by internal wall corrosion.

3.3. Leakage monitoring based on hoop strain

Fluids suddenly escape from the leakage point when leakages take place, leading to the loss of the fluid and the pressure drops. Then the negative pressure wave (NPW) generates and propagates toward to the upstream and downstream at a certain speed [56], causing the sudden drop of inner pressure. In this condition, where R, δ and E in Eq. (1) are considered to be constant, the hoop strain ε is proportional to the internal pressure P. According to this principle, hoop strain can be used to detect the internal pressure variation caused by pipeline leakages.

4. Calibration test

In the corrosion and leakage simulation tests, a polyimide-coated optical fiber was used. The protective coatings of optical fiber will absorb a portion of the strain and lead to the measurement error [57]. Therefore, a calibration test was conducted to test the performance of the polyimide-coated optical fiber in strain measurement.

The test was carried out on a steel plate, of which the cross section is a rectangle (30 mm × 5.7 mm). Before bonding the optic fiber, the surface of the steel plate was cleaned carefully. Then the polyimide-coated optical fiber was bonded continuously along the central line of the steel plate with length 200 mm. Three FBG strain sensors (S1, S2 and S3) were employed in the tests, providing a comparison to the results measured by polyimide-coated optical fiber. The three FBG sensors were bonded to the steel plate at the same interval of 50 mm and arranged in a straight line near the optical fiber with the distance of 2 mm. The position of optical fiber and FBG sensors are displayed in Fig. 1. Tensile tests of the steel plate were carried out on a universal material testing machine shown in Fig. 1. In the tests, the steel plate was loaded continuously from 0 kN to 24 kN at an interval of 2 kN. The Luna ODiSI system was employed to measure the distributed strain of OFS and the Micron Optics SM130 was used to demodulate the wavelength of the FBG sensors.

Fig. 2 displays the distributed strain measured by DOFS. For a steel plate with the same cross section, the strain distribution under each loading step is a theoretical horizontal line. It can be observed from Fig. 2 that the measured strain distribution accords with the theoretical strain distribution of the steel plate under the tensile load.

Fig. 3 shows the comparison of the strain variation measured by the distributed optical fiber sensors and the FBG strain sensors at location of S1, S2 and S3 (shown in Fig. 1) respectively, when the steel plate was subjected to stepwise loading. The results illustrate that there were excellent agreements between the strain measurement obtained by the fiber sensor and the FBG strain sensors for single-point measurement, indicating the DOFS is suitable for the continuous strain measurement in time domain. The calibration tests demonstrate that the polyimide-coated optical fiber has excellent performance in the distributed strain measurement.

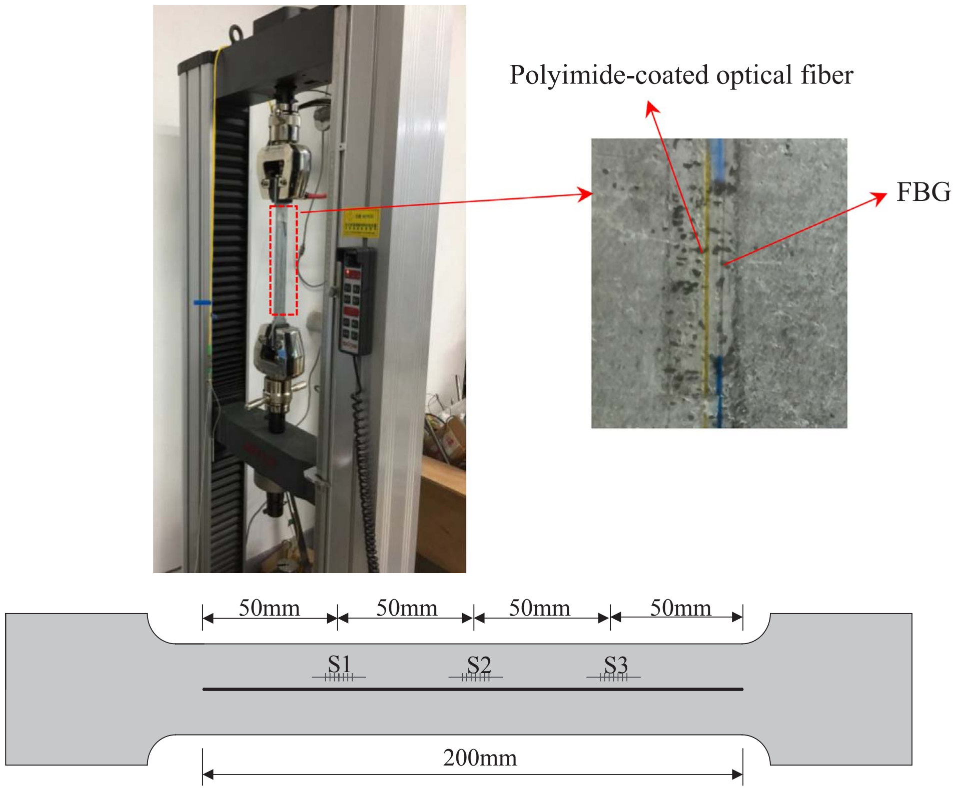

Fig. 1. Calibration experiment using an universal material test machine.

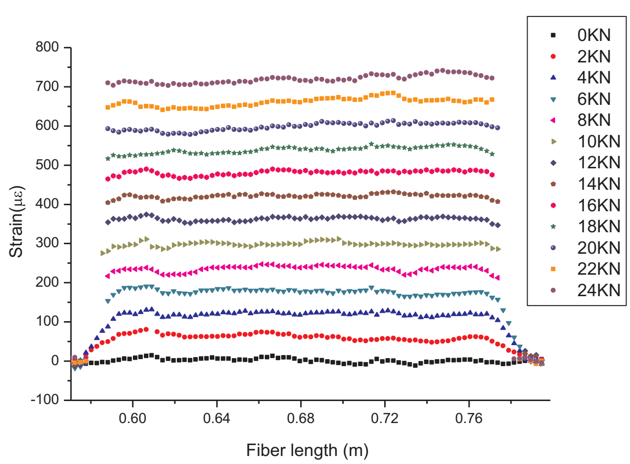

Fig. 2. Strain distribution measured by DOFS.

5. Pipeline corrosion monitoring test

In this case study, a corrosion process was simulated and a sensor array composed of DOFS s were used to monitor the corrosion process. Based on the sensor array, a hoop strain nephogram was proposed to identify corrosion, localize corrosion and assess corrosion level simultaneously.

5.1. Test set-up

The pipe model shown in Fig. 4 is a steel pipe with 219 mm outer diameter and 12 mm wall thickness. Both two ends of this model were sealed with flanges. The internal wall was painted with anti-corrosive coatings. While a region with an axial length of 150 mm and a circumferential length of 100 mm was not painted, it was set as a local corrosion region. The model was filled with salt water (concentration of 10%) to provide a corrosive environment. A steel bar, which was connected to the negative pole of a direct current power, was put into the pipe model and immersed into the salt water. Meanwhile, the pipe model was connected to the positive pole of the direct current power. Therefore, the steel pipe, the steel bar, the salt water and the direct current power composed an electrolytic cell which can accelerate the speed of corrosion. It should be noted that the steel bar was close to the corrosion region but did not touch the internal wall of the pipe. In this way, the corrosion rate of the corrosion region can be accelerated. Meanwhile, the other region avoids being corroded.

In this test, eight polyimide coated optical fibers (1#–8#) were bonded to the pipe surface at the same interval of 20 mm. Before bonding the optical fiber, electric sander and abrasive paper were used to polish the out surface of the pipe model. After polishing, the surface was cleaned by cotton immersed in alcohol. Then the optical fibers were adhered along the circumferential direction and covered the whole circle of the pipe model. The location of optical fibers is indicated in Fig. 5.

In order to acquire the corrosion development process, distributed hoop strain data was measured by the ODiSI system every 5 h. When it measured the hoop strain, the electrolytic cell stopped working and the steel bar was taken out of the model. Then a water pump was applied to provide pressurized condition (1.0 MPa) to simulate the working environment of practical pipeline.

5.2. Test results

Fig. 6 shows the distributed strain profile of sensor 5# (see Fig. 5) measured at different times but under the same internal pressure. When the pipe model was not subjected to corrosion, the hoop strain distribution along the whole circle fluctuated around the value of 30 με. However, after 50 h, strain concentrated on a segment from 0.2 m to 0.40 m where the local corrosion area is located at, it indicates that the corresponding internal wall of this area has been corroded. Comparing the test results of 0 h, 50 h, 100 h, 150 h and 200 h, it can be seen that

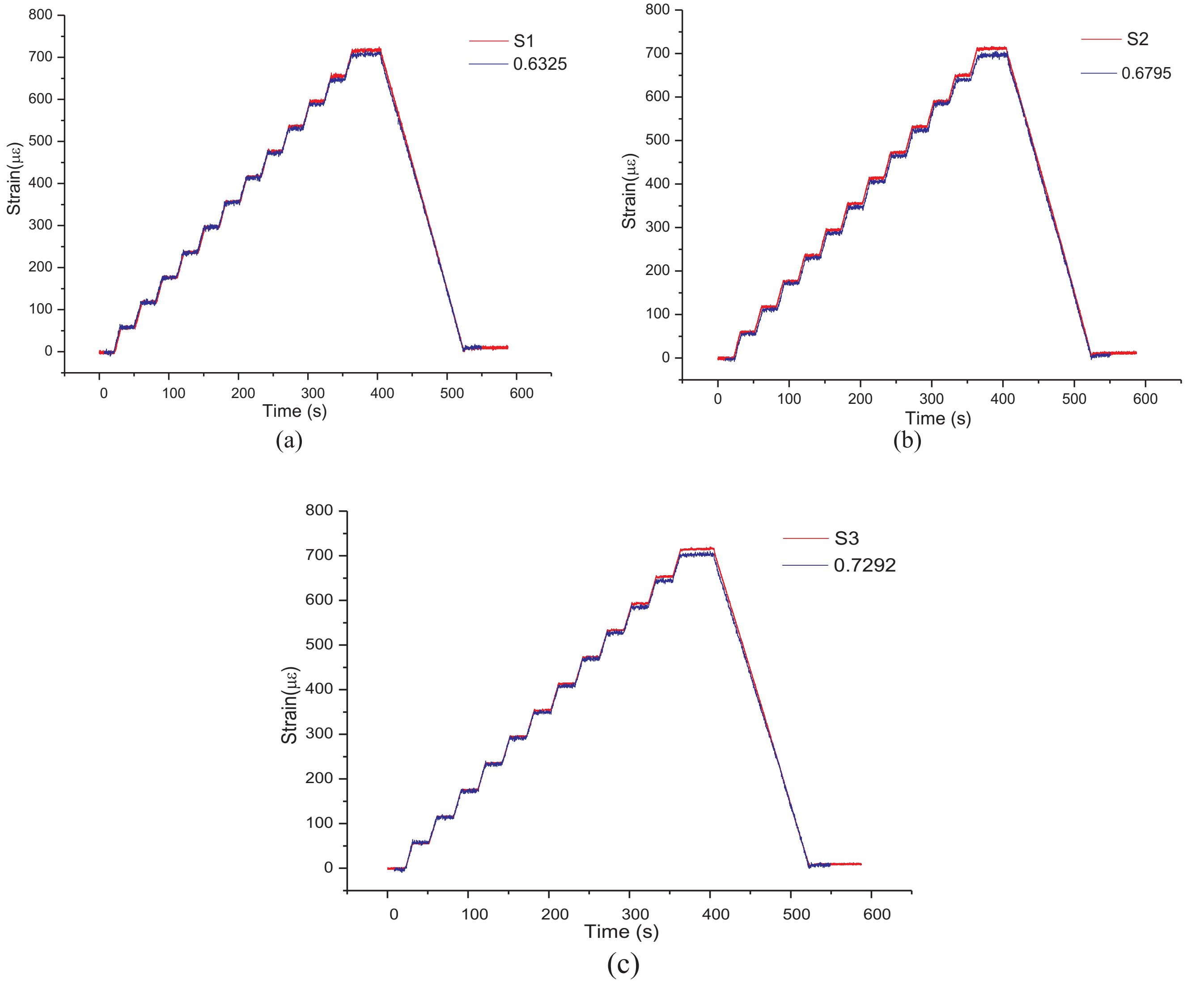

Fig. 3. Strain variation of discrete points measured by DOFS and FBG when subject to increasing tensile load. (a) Point S1, (b) point S2 and (c) point S3.

the hoop strain increases since the internal wall has been continuously corroded. Test results demonstrate that corrosion can be detected based on hoop strain distribution measured by the DOFS.

According to the distributed hoop strain of one DOFS, the local corrosion scope along the circumferential direction can be identified. However, the corrosion scope along the pipe axial direction cannot be detected by one DOFS. Therefore, a hoop strain nephogram is proposed to show the corrosion location and corrosion level in case that corrosion promotes a change in the pipe internal wall. The equidistant DOFSs mounted on the pipe surface compose a sensor array. With the ability of

Fig. 4. Corrosion test pipe and direct current power.

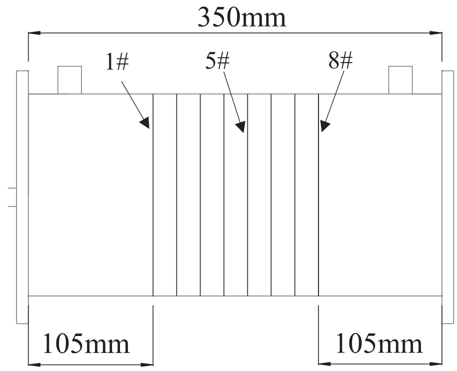

Fig. 5. Schematic diagram of pipe model and the location of optical fiber.

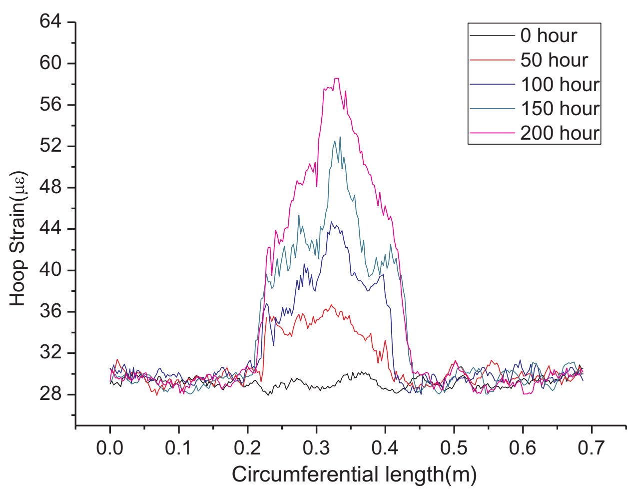

Fig. 6. Hoop strain distribution measured by one DOFS.

measuring the hoop strain from the full surface of the pipe, the sensor array is used to create the hoop strain nephogram. Note that the hoop strain measured by one DOFS can be used to generate the hoop strain nephogram directly since the ODiSI system can achieve 2.56 mm sensor spacing. However, the distance between two neighboring sensors is 20 mm. Therefore, the interpolation method was used to calculate the strain between the two adjacent sensors. For the hoop strain nephogram, the circumferential range is the entire circumference (687.7 mm) and the axial range is expanded 20 mm at both end of the sensor array. An ultrasonic based thickness tester was used to detect the wall thickness distribution. The wall thickness data was also made into a wall thickness distribution nephogram, used as a reference to the hoop strain nephogram.

When the pipe was corroded after 100 h, data measured by the sensor array was utilized to create a two-dimensional hoop strain nephogram and a three-dimensional hoop strain nephogram, shown in Fig. 7(a) and (b) respectively. Fig. 7(a) clearly presents that there is a strain concentration area (circumferential direction: from 0.2 m to 0.4 m; axial direction: from 0.06 m to 0.14 m) on the hoop strain nephogram. This is attributed to the reason that under a constant pressure within the pipe, larger hoop strain appears in the corrosion region where a certain percentage of wall thickness loses. The location of hoop strain concentration area displayed in Fig. 7(a) matches the wall thickness reduction area shown in Fig. 8(a), demonstrating that the hoop strain nephogram can present the corrosion area clearly. However, the boundary condition of corrosion area brings about the fact that the strain concentration area is a little larger than the wall thickness reduction area. Fig. 7(b) displays that an red area with large hoop strain appears in the center of the corrosion nephogram. From the wall thickness nephogram presented in Fig. 8, the wall thickness of red area shown in Fig. 7(b) is less than 9 mm, that means 3 mm wall thickness has been corroded. It can be concluded the corrosion degree can be reported by the hoop strain nephogram intuitively.

When the pipe model was corroded 200 h, hoop strain data and wall thickness data were measured and used to create the hoop strain nephogram (displayed in Fig. 9) and wall thickness nephogram (displayed in Fig. 10) respectively. Test results in this case demonstrate that the hoop strain nephogram can report the corrosion scope and corrosion level effectively. Compared with Fig. 7(a), Fig. 9(a) shows that after being corroded 200 h, the hoop strain concentration area extends, and also the hoop strain increases. In contrast with Figure (b), the wall thickness nephogram shown in Fig. 10 also presents that corrosion makes the wall thickness decrease 2 mm and also makes the corrosion area expand.

The results conclude that the hoop strain nephogram has good performance in identifying corrosion scope, localizing corrosion location and evaluating corrosion degree. Additionally, the safety state of the corrosion region can be evaluated using the hoop strain nephogram.

6. Pipeline leakage monitoring test

Even though internal corrosion and leakage may occur on one pipeline, but corrosion and leakage are two different events. For time domain characters of these two signals, corrosion is a steady-state process, while leakage is a transient process. Additionally, it is difficult to simulate NPW in the short corrosion pipeline model. Thus another longer pipeline model was built to simulate leakage.

6.1. Test set-up

The pipeline model (displayed in Fig. 11) employed to simulate leakage was consisted of a series of PVC pipe sections connected

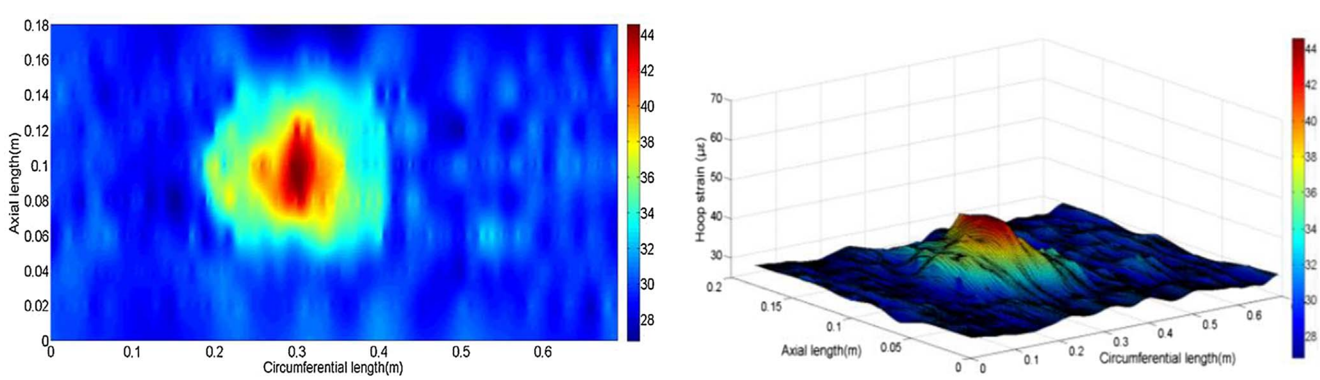

(a) (b)

Fig. 7. Hoop strain nephogram when the pipe was corroded 100 h. (a) 2D and (b) 3D.

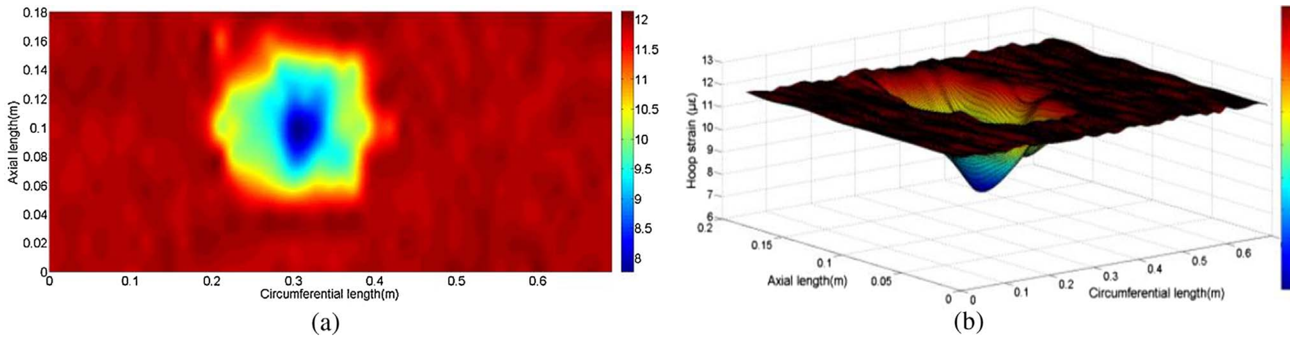

Fig. 8. Wall thickness nephogram when the pipe was corroded 100 h. (a) 2D and (b) 3D.

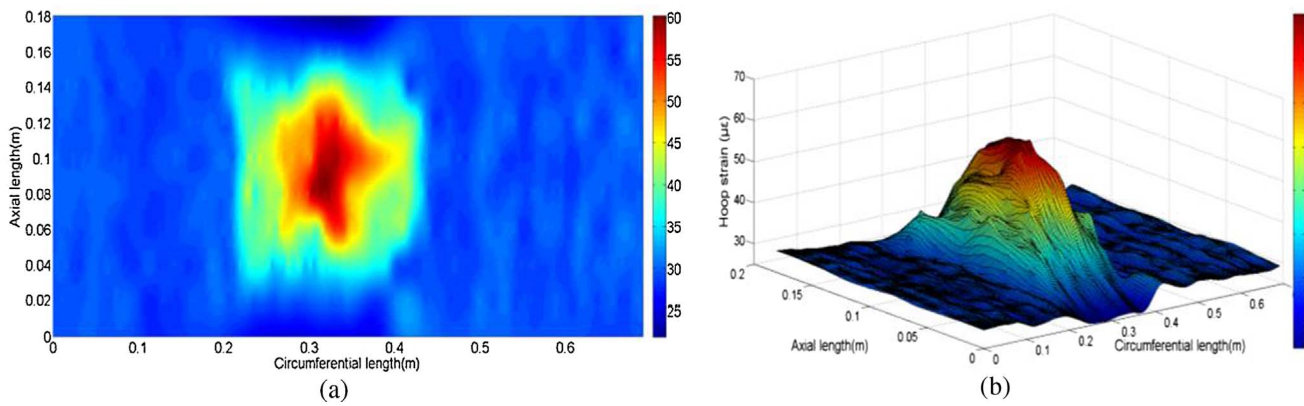

Fig. 9. Hoop strain nephogram when the pipe was corroded 200 h. (a) 2D and (b) 3D.

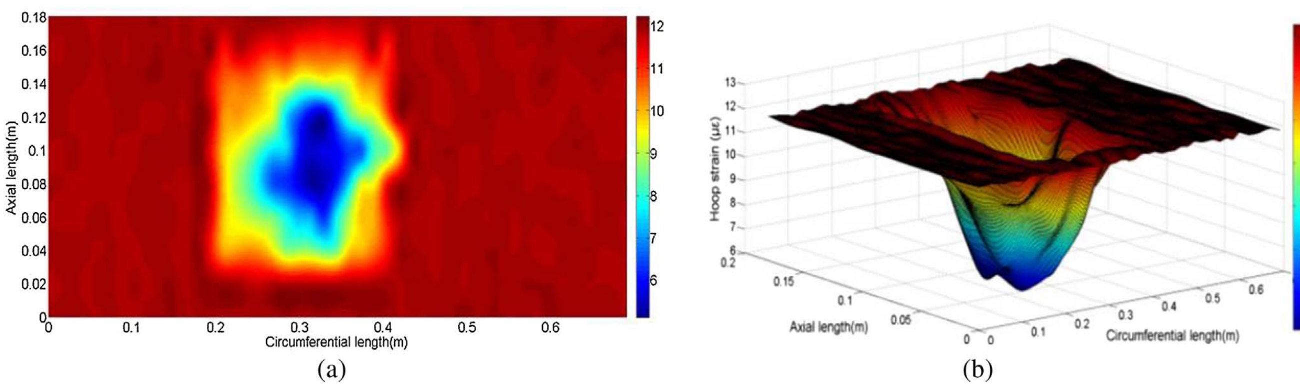

Fig. 10. Wall thickness nephogram when the pipe was corroded 200 h. (a) 2D and (b) 3D.

together to compose a pipeline with a total length of 57.2 m. Seven manually controllable leakage valves (L1–L7) were installed every 8.2 m along the pipeline (see Fig. 11). Seven test segments S1–S7 of one polyimide-coated optical fiber were bonded to the pipeline model with one whole circle to measure the hoop strain variation during the leakage process. While the rest segments of the optic fiber were not bonded to the pipeline model. The unbonded segment of the optic fiber which is closed to the test segment is set as the reference to compensate the change in temperature.

Before simulating leakage process, pipeline model was pressurized to 20 kPa using an air compressor. Then the valve was opened rapidly to produce a leakage event to the pipeline model. During the leakage test, the inner pressure dropped from 20 kPa to 0 kPa. The ODiSI system was used to measure the strain variation at a frequency of 100 Hz throughout the leakage simulation test.

6.2. Test results

For the distributed strain sensing, any point along the optical fiber bonded to the pipe can be used to investigate the dynamic response of the leakage process. Strain variation during the leakage process of a specific point (in the middle of S2) was extracted and shown in Fig. 12. The results indicate that the hoop strain fluctuates at the value of 0 με before the leakage occurrence. Then, the hoop strain suddenly descended when the leakage happened. This can be attributed to the NPW, which propagates along the pipeline model and causes the inner pressure reduced upon the arrival of the NPW to its location, simultaneously resulting in the hoop strain slump promptly. This phenomenon can be considered as an important indication for pipeline leakage happening.

In order to show the hoop strain variation of different location along the pipeline, hoop strain response of three points extracted from S1, S4 and S7 respectively were displayed in Fig. 13. By comparing the hoop strain time history of different location, it presents that S1 is the first sensor to detect the turning point, while S7 is the last one to detect the

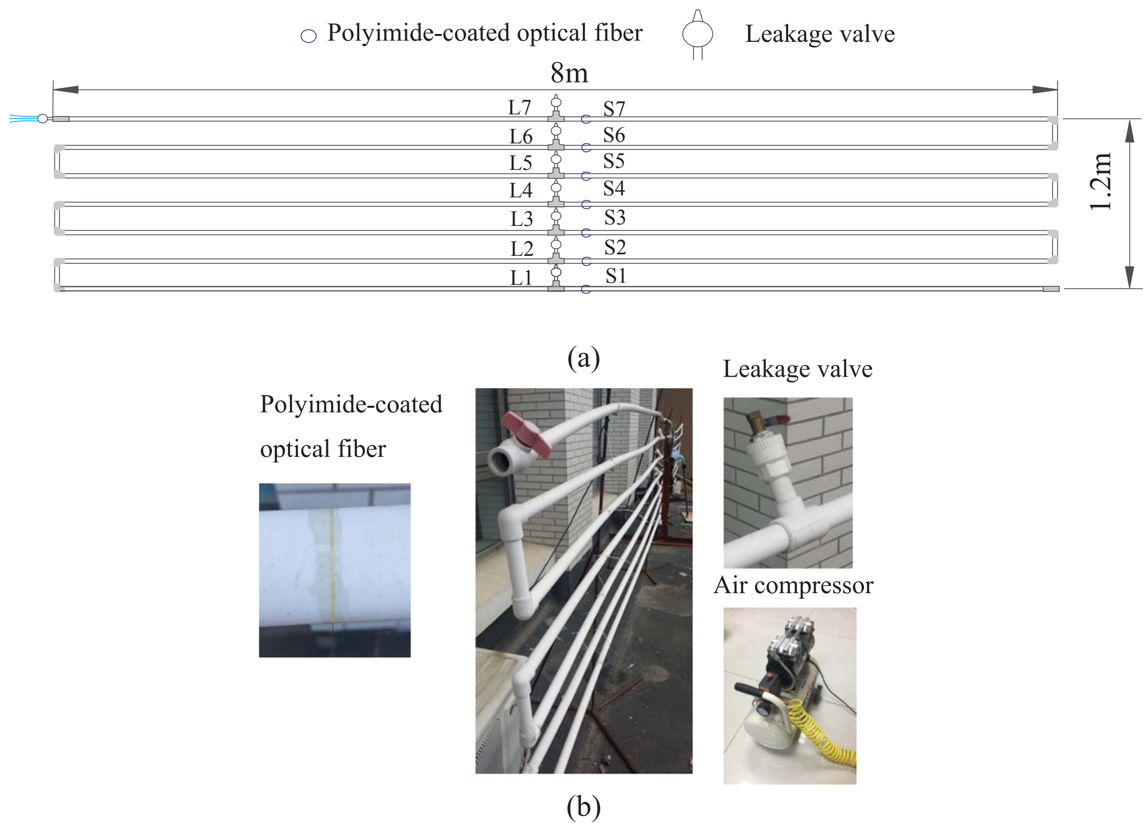

Fig. 11. Diagram of pipeline model. (a) Pipeline model schematic. (b) Diagram of pipeline model.

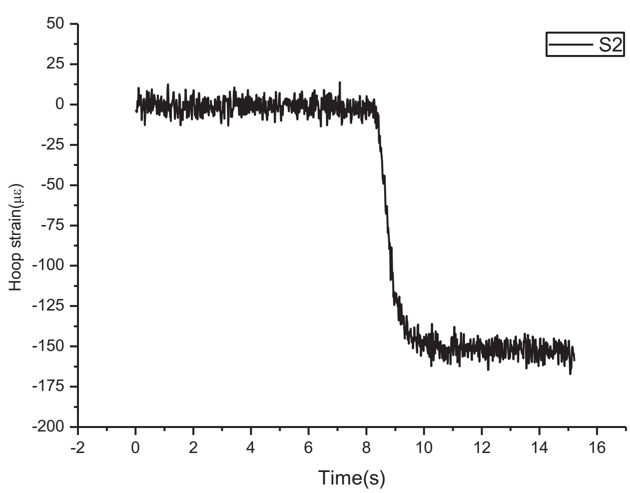

Fig. 12. Hoop strain responses induced by leakage point L2.

turning point. This phenomenon demonstrates that NPW propagates along the pipeline model at a certain speed. Thus, the sensor closer to the leakage point experienced the hoop strain sooner than the other sensors. The time when a turning point appears is the arrival time of NPW. Based on the difference in time it takes for the NPW to reach the OFS, the leakage location can be calculated. However, limited by the sampling frequency of the ODiSI system, the precision of leakage localization is not high. Therefore, in the next stage, a more accurate leakage localization method will be studied. The results obtained in this case study conclude that by detecting the features in hoop strain time history, it is possible to monitor the appearance of leakage.

7. Conclusions

The OFDR technique provides a unique capability to measure the distributed strain in high spatial resolution and high precision, as well as the dynamic measurement. Based on the OFDR technique, a new application was proposed to monitor pipeline corrosion and leakage by measuring the distributed hoop strain along the outer surface of the pipeline. To verify the feasibility of this method, a series of simulating tests were conducted. From the simulation tests, the following conclusions can be obtained:

(1) Hoop strain is a key parameter and can be used to monitor pipeline corrosion and leakage.
(2) The hoop stain nephogram has good performance in identifying the corrosion scope, evaluating corrosion degree and localizing corrosion location.
(3) Pipeline leakage induces a turning point and can be detected by the OFS.

All the results show that the OFDR based distributes strain measurement technique offers great potential in pipeline safety monitoring that allows high efficiency and accuracy systems to be achieved. However, this study is still in a very early stage, and more investigations should be conducted, such as a more accurate leakage localization method.

Acknowledgements

This work has been supported by the National Key Research and Development Program of China (Grant No. 2016YFC0701107), the Fund of the National Natural Science Foundation of China (Grant No. 51421064, 51327003, 51678109 and 51608094). These grants are greatly appreciated.

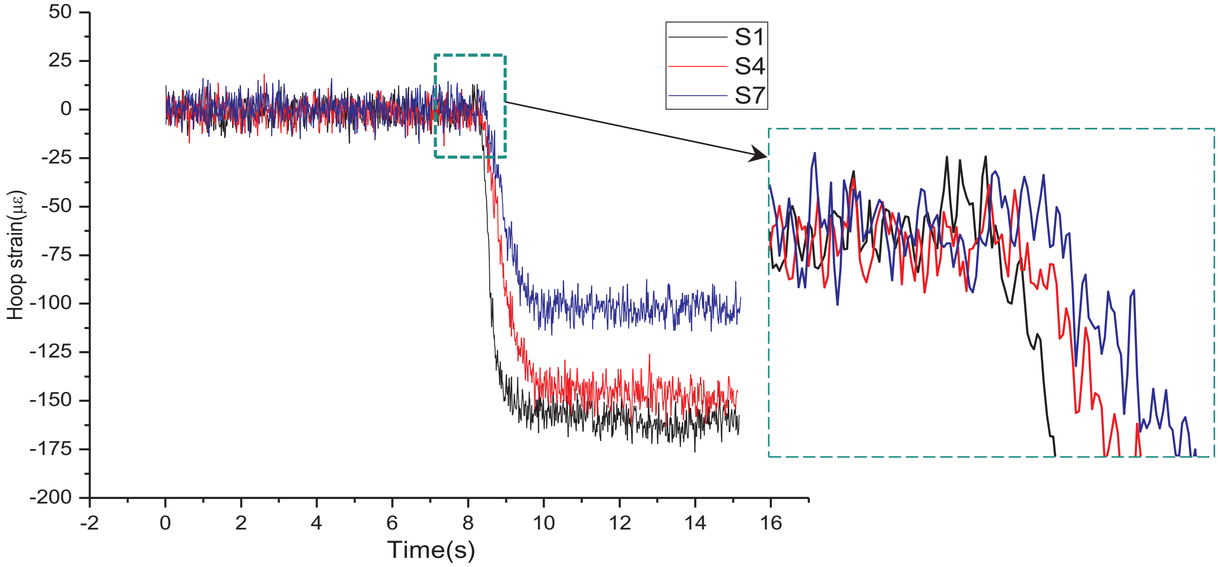

Fig. 13. Hoop strain responses of different location induced by leakage point L2.

References

[1] O.M. Aamo, Leak detection, size estimation and localization in pipe flows, IEEE Trans. Autom. Control 61 (1) (2016) 246–251.
[2] Y.A. Khulief, A. Khalifa, R.B. Mansour, M.A. Habib, Acoustic detection of leaks in water pipelines using measurements inside pipe, J. Pipeline Syst. Eng. Pract. 3 (2) (2011) 47–54.
[3] C. Beck, J. Grieser, M. Kottek, F. Rubel, B. Rudolf, Characterizing global climate change by means of Köppen climate classification, Klimastatusbericht 51 (2005) 139–149.
[4] B.N. Shivananju, M. Kiran, S.P. Nithin, M.J. Vidya, G.M. Hegde, S. Asokan, Real time monitoring of petroleum leakage detection using etched fiber Bragg grating, in: International Conference on Optics in Precision Engineering and Nanotechnology (icOPEN2013), International Society for Optics and Photonics, 2013, pp. 876922-876922-5.
[5] L. Sun, X.S. Zhang, Q.Q. Sun, B.W. Chen, Study on failure pressure of corroded submarine pipeline under earthquake, in: Applied Mechanics and Materials, vol. 71, Trans Tech Publications, 2011, pp. 1703–1706.
[6] H.A. Kishawy, H.A. Gabbar, Review of pipeline integrity management practices, Int. J. Press. Vessels Pip. 87 (7) (2010) 373–380.
[7] P. Huthwaite, R. Ribichini, P. Cawley, M.J. Lowe, Mode selection for corrosion detection in pipes and vessels via guided wave tomography, IEEE Trans. Ultrason. Ferroelect. Freq. Control 60 (6) (2013) 1165–1177.
[8] H. Li, P. Zhang, G. Song, D. Patil, Y. Mo, Robustness study of the pounding tuned mass damper for vibration control of subsea jumpers, Smart Mater. Struct. 24 (9) (2015) 095001.
[9] J. Zhou, L. Sun, H. Li, Study on dynamic response measurement of the submarine pipeline by full-term FBG sensors, Sci. World J. 2014 (2014).
[10] M.R.U. Kawsar, S.A. Youssef, M. Faisal, A. Kumar, J.K. Seo, J.K. Paik, Assessment of dropped object risk on corroded subsea pipeline, Ocean Eng. 106 (2015) 329–340.
[11] R.C. Tennyson, W.D. Morison, Long gage-length optic sensors for monitoring pipeline integrity, in: Proc. of SPIE2006, 6167, pp. 1–13.
[12] Z. Wang, Q. Cao, N. Luan, L. Zhang, Development of an autonomous in-pipe robot for offshore pipeline maintenance, Ind. Robot: Int. J. 37 (2) (2010) 177–184.
[13] M.H. Skjelvareid, Y. Birkelund, Y. Larsen, Internal pipeline inspection using virtual source synthetic aperture ultrasound imaging, Ndt & E Int. 54 (2013) 151–158.
[14] Z. Sun, P. Wang, M.C. Vuran, M.A. Al-Rodhaan, A.M. Al-Dhelaan, I.F. Akyildiz, MISE-PIPE: magnetic induction-based wireless sensor networks for underground pipeline monitoring, Ad Hoc Netw. 9 (3) (2011) 218–227.
[15] D. Inaudi, B. Glisic, Long-range pipeline monitoring by distributed fiber optic sensing, J. Pres. Vessel Technol. 132 (1) (2010) 011701.
[16] S.Z. Yan, L.S. Chyan, Performance enhancement of BOTDR fiber optic sensor for oil and gas pipeline monitoring, Opt. Fiber Technol. 16 (2) (2010) 100–109.
[17] G. Du, Q. Kong, T. Lai, G. Song, Feasibility study on crack detection of pipelines using piezoceramic transducers, Int. J. Distrib. Sens. Netw. 9 (10) (2013) 631715.
[18] Q. Feng, Q. Kong, L. Huo, G. Song, Crack detection and leakage monitoring on reinforced concrete pipe, Smart Mater. Struct. 24 (11) (2015) 115020.
[19] J. Zhu, L. Ren, S.C. Ho, Z. Jia, G. Song, Gas pipeline leakage detection based on PZT sensors, Smart Mater. Struct. 26 (2) (2017) 025022.
[20] D. Ozevin, J. Harding, Novel leak localization in pressurized pipeline networks using acoustic emission and geometric connectivity, Int. J. Press. Vessels Pip. 92 (2012) 63–69.
[21] C. Xu, P. Gong, J. Xie, H. Shi, G. Chen, G. Song, An acoustic emission based multi-level approach to buried gas pipeline leakage localization, J. Loss Prev. Process Ind. 44 (2016) 397–404.
[22] Z. Qu, H. Feng, Z. Zeng, J. Zhuge, S. Jin, A SVM-based pipeline leakage detection and pre-warning system, Measurement 43 (4) (2010) 513–519.
[23] L. Ni, J. Jiang, Y. Pan, Leak location of pipelines based on transient model and PSO-SVM, J. Loss Prevent. Process Ind. 26 (6) (2013) 1085–1093.
[24] G. Ye, R.A. Fenner, Kalman filtering of hydraulic measurements for burst detection in water distribution systems, J. Pipeline Syst. Eng. Practice 2 (1) (2010) 14–22.
[25] X. Hong, G. Song, J. Ruan, Z. Zhang, S. Wu, G. Liu, Active monitoring of pipeline tapered thread connection based on time reversal using piezoceramic transducers, Smart Struct. Syst. 18 (4) (2016) 643–662.
[26] G. Du, Q. Kong, F. Wu, J. Ruan, G. Song, An experimental feasibility study of pipeline corrosion pit detection using a piezoceramic time reversal mirror, Smart Mater. Struct. 25 (3) (2016) 037002.
[27] D. Covas, H. Ramos, B.A. Almeida, Impulse response method for solving hydraulic transients in viscoelastic pipes, in: XXXI IAHR Congress, Seoul, South Korea, Sept. 2005, pp. 11–16.
[28] G. Du, Q. Kong, H. Zhou, H. Gu, Multiple cracks detection in pipeline using damage index matrix based on piezoceramic transducer-enabled stress wave propagation, Sensors 17 (8) (2017) 1812.
[29] L. Zou, O. Sezerman, W. Revie, Pipeline corrosion monitoring by fiber optic distributed strain and temperature sensors, in: NACE International Corrosion Conference and Expo., 2008.
[30] P.L. Fuhr, D.R. Huston, Multiplexed fiber optic pressure and vibration sensors for hydroelectric dam monitoring, Smart Mater. Struct. 2 (4) (1993) 260.
[31] E. Reynders, G.D. Roeck, P. Gundes Bakir, C. Sauvage, Damage identification on the Tilff Bridge by vibration monitoring using optical fiber strain sensors, J. Eng. Mech. 133 (2) (2007) 185–193.
[32] J. Gao, B. Shi, W. Zhang, H. Zhu, Monitoring the stress of the post-tensioning cable using fiber optic distributed strain sensor, Measurement 39 (5) (2006) 420–428.
[33] M.A. Soto, G. Bolognini, F. Di Pasquale, Long-range simplex-coded BOTDA sensor over 120 km distance employing optical preamplification, Opt. Lett. 36 (2) (2011) 232–234.
[34] X. Bao, L. Chen, Recent progress in distributed fiber optic sensors, Sensors 12 (7) (2012) 8601–8639.
[35] L. Ren, T. Jiang, D.S. Li, P. Zhang, H.N. Li, G.B. Song, A method of pipeline corrosion detection based on hoop-strain monitoring technology, Struct. Control Health Monit. (2016).
[36] L. Sun, C. Chen, Q.Q. Sun, Experimental and finite element analyses on the corrosion of underground pipelines, Sci. Chin. Technol. Sci. 58 (6) (2015) 1015–1020.
[37] G. Peng, J. He, S. Yang, W. Zhou, Application of the fiber-optic distributed temperature sensing for monitoring the liquid level of producing oil wells, Measurement 58 (2014) 130–137.
[38] S. Uchida, E. Levenberg, A. Klar, On-specimen strain measurement with fiber optic distributed sensing, Measurement 60 (2015) 104–113.
[39] P. Rajeev, J. Kodikara, W.K. Chiu, T. Kuen, Distributed optical fibre sensors and their applications in pipeline monitoring, in: Key Engineering Materials, vol. 558, Trans Tech Publications, 2013, pp. 424–434.
[40] T. Jiang, L. Ren, Z.G. Jia, D.S. Li, H.N. Li, Pipeline internal corrosion monitoring based on distributed strain measurement technique, Struct. Control Health Monit. (2017).
[41] L. Zou, G.A. Ferrier, S. Afshar, Q. Yu, L. Chen, X. Bao, Distributed Brillouin scattering sensor for discrimination of wall-thinning defects in steel pipe under internal pressure, Appl. Opt. 43 (7) (2004) 1583–1588.
[42] K. Alhandawi, N. Vahdati, O. Shiryayev, L. Lawand, Corrosion monitoring along infrastructures using distributed fiber optic sensing, in: Proceedings of the SPIE Smart Structures and Materials + Nondestructive Evaluation and Health Monitoring, Las Vegas, NV, USA, 20–24 March 2016.

[43] J.F. Martins-Filho, E. Fontana, J. Guimaraes, D.F. Pizzato, I.S. Coelho, Fiber-optic-based corrosion sensor using OTDR, IEEE Sens. (2007) 1172–1174.
[44] W. Li, X. Bao, high spatial resolution distributed fiber optic technique for strain and temperature measurements in concrete structures, in: Proceedings of the International Workshop on Smart Materials, Structures NDT in Canada 2013 Conference & NDT for the Energy Industry, Calgary, Canada.
[45] T. Jiang, L. Ren, Z. Jia, D. Li, H. Li, Application of FBG based sensor in pipeline safety monitoring, Appl. Sci. 7 (6) (2017) 540.
[46] J.M. Rajtar, R. Muthiah, Pipeline leak detection system for oil and gas flowlines, J. Manuf. Sci. Eng., Trans. ASME 119 (1) (1997) 105–109.
[47] M. Niklès, B.H. Vogel, F. Briffod, S. Grosswig, F. Sauser, S. Luebbecke, T. Pfeiffer, Leakage detection using fiber optics distributed temperature monitoring, in: Smart Structures and Materials, International Society for Optics and Photonics, 2004, pp. 18–25.
[48] F. Tanimola, D. Hill, Distributed fibre optic sensors for pipeline protection, J. Nat. Gas Sci. Eng. 1 (4) (2009) 134–143.
[49] P.S. Murvay, I. Silea, A survey on gas leak detection and localization techniques, J. Loss Prev. Process Ind. 25 (6) (2012) 966–973.
[50] L. Wong, W.K. Chiu, J. Kodikara, Using distributed optical fibre sensor to enhance structural health monitoring of a pipeline subjected to hydraulic transient excitation, Struct. Health Monit. 1475921717691036 (2017).
[51] M. Froggatt, J. Moore, High resolution strain measurement in optical fiber with Rayleigh scatter, Appl. Opt. 37 (1998) 1735–1740.
[52] M. Froggatt, B. Soller, D. Gifford, M. Wolfe, Correlation and keying of Rayleigh scatter for loss and temperature sensing in parallel optical networks, in: Optical Fiber Communication Conference, Optical Society of America, 2004, PD17.
[53] B.J. Soller, M. Wolfe, M.E. Froggatt, Polarization resolved measurement of Rayleigh backscatter in fiber-optic components, in: National Fiber Optic Engineers Conference, Optical Society of America, 2005, NWD3.
[54] Luna ODiSI Optical distributed sensor interrogator user guide.
[55] W. Li, L. Chen, X. Bao, Compensation of temperature and strain coefficients due to local birefringence using optical frequency domain reflectometry, Opt. Commun. 311 (2013) 26–32.
[56] Z.G. Jia, L. Ren, H.N. Li, S.C. Ho, G.B. Song, Experimental study of pipeline leak detection based on hoop strain measurement, Struct. Control Health Monit. 22 (5) (2015) 799–812.
[57] F. Ansari, Y. Libo, Mechanics of bond and interface shear transfer in optical fiber sensors, J. Eng. Mech. 124 (4) (1998) 385–394.